SPEEDAM 2010
International Symposium on Power Electronics,
Electrical Drives, Automation and Motion

Determination of Single Phase Induction Motor Parameters

V. Hrabovcova, L. Kalamen, P. Sekerak and P. Rafajdus
Department of Power Electrical Systems, University of Žilina, Univerzitná 1, 010 26 Žilina, Slovakia
Valeria.Hrabovcova@fel.uniza.sk, Pavol.Rafajdus@kves.uniza.sk
Peter.Sekerak@kves.uniza.sk, Lukas.Kalamen@kves.uniza.sk

***Abstract* — Measurement and determination of parameters of single-phase induction machines is quite a difficult task in comparison with symmetrical three-phase induction machines. This paper describes three different methods for parameter determination of single-phase machines. Conventional (classical) method, usually used for three-phase machines, is complemented by Suhr's and two-phase method. Furthermore, measured parameters are supported and confirmed by means of finite element method and calculations based on electrical machine design. The gained parameters are used in simulation model of single-phase machine in steady-state conditions in stable region and subsequently compared with measurement on a small real motor. Simulation results show a good agreement with behavior of a real machine. Finally, an easy method for the replacement of two-phase supply is described.**

***Index Terms* — Single-phase induction motor, two-phase induction motor, measurement, machine parameters, finite element method**

I. Introduction

Single-phase induction machines (SPIM) have been used for a long time because of their simple construction and because the single-phase power supply is available in almost every household. However, this advantage is compensated by minor utilization of the machine and its complicated start-up.

Single-phase power supplied to single phase winding is a source of pulsating field in a machine that can be resolved into two equal revolving fields rotating in opposite direction. Thus, the machine does not produce starting torque (Fig. 1).

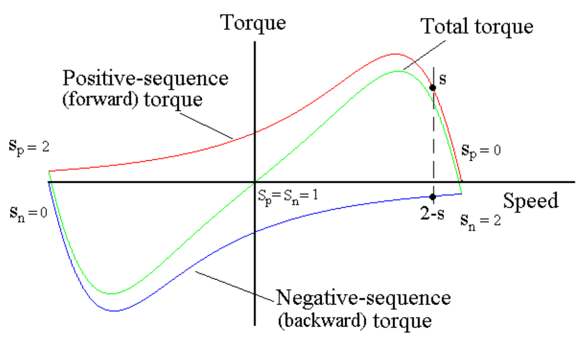

Fig. 1. Torque - speed characteristic for SPIM induced positive and negative sequence components.

This work was supported by VEGA (Scientific Grant Agency of the Slovak Republic) No. 1/0470/09

After the rotor starts rotating in one direction by a mechanical impulse, the field rotating in direction of the rotation of rotor starts to dominate over backward rotating field and motor will run up. Torque of backward rotating field will decrease with the increasing rotor speed and at nominal speed it is only a very small fraction of total torque.

As can be seen in the Fig. 1 there is no starting torque which is the biggest disadvantage of SPIM. Thus, SPIM with only one stator winding (see Fig. 2a) are not manufactured. Usually an auxiliary winding with different impedance shifted in space by 90° is wound to ensure the run-up and improve the starting up performance of SPIM (Fig. 2b).

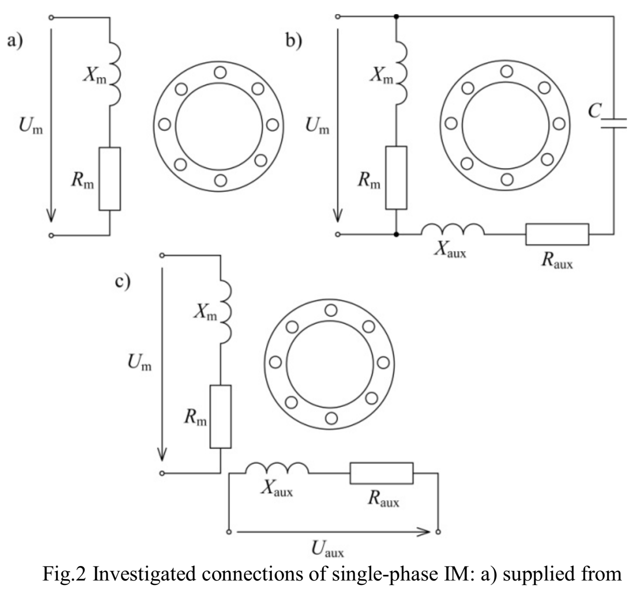

Fig.2 Investigated connections of single-phase IM: a) supplied from main phase b) with capacitor c) two-phase supply

There are various methods for running-up SPIM with auxiliary winding. The most commonly used method is the one with permanently connected starting-up capacitor (Fig. 2b). With respect to the current of the main winding the current in auxiliary winding is now shifted by almost 90° and leading the main winding current. The field produced by both windings is no more pulsating and the machine produces starting torque. However, field produced in machine air gap is not symmetrical like in three-phase machines but an elliptical one which means that the magnitude of magnetic field density along the machine air gap is non-uniform (Fig. 3). Such field is a

978-1-4244-4987-3/10/$25.00 ©2010 IEEE

source of increased noise and vibrations due to radial forces affecting the stator boring [1].

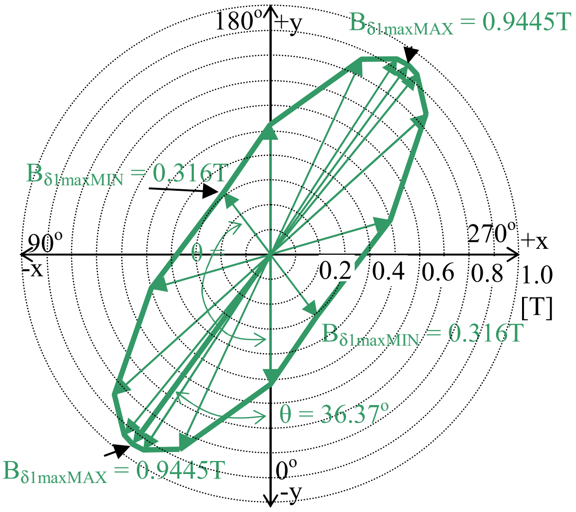

Fig. 3. The space distribution of the $B_{\delta 1max}$ in the air-gap of the investigated machine with capacitor.

Permanent progress in the field of power electronic devices has given a rise to two-phase induction machines (TPIM). These machines have two equal stator windings spatially shifted by 90° (Fig. 2c). Supply is carried out by two-phase power converter with currents shifted by 90° in time. By means of this supply a waveform of flux density rotating in the air gap, similar to that of the field in three-phase machines, is produced and vibrations and unfavourable noise are thus suppressed. Due to smaller amount of power switches in converters for TPIM and its simpler construction, such machines are quite economical. Of course, their torque and output power are proportional to number of phases. This paper deals with SPIM.

An equivalent circuit of SPIM in steady-state condition can be created if rotor parameters are equally divided between forward and backward components of rotating field. Forward resistance component is represented as $0{,}5R'_r/s$, backward component as $0{,}5R'_r/(2\text{-}s)$, which can be seen in Fig. 4 and justified by the Fig. 1. Magnetizing reactance X_μ is divided into two components as well.

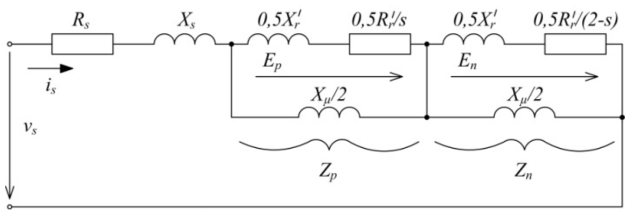

Fig. 4. Equivalent circuit of single-phase motor.

From equivalent circuit the rotor impedance belonging to forward (subscript "p" as positive) and backward (subscript "n" as negative) rotating fields can be calculated as:

$$Z_{rp} = 0{,}5X_r' + \frac{0{,}5R_r'}{s} \quad (1)$$

$$Z_{rn} = 0{,}5X_r' + \frac{0{,}5R_r'}{2-s} \quad (2)$$

where R_r' and X_r' are rotor resistance and reactance referred to the stator side.

Together with magnetizing reactance X_m it results in total parallel impedances:

$$Z_p = \frac{Z_{rp}0{,}5X_m}{Z_{rp}+0{,}5X_m} \quad (3)$$

$$Z_n = \frac{Z_{rn}0{,}5X_m}{Z_{rn}+0{,}5X_m} \quad (4)$$

After adding the stator impedance $Z_s=R_s+jX_s$ we obtain the input impedance Z_{in}. Afterwards, input current I_s can be calculated as ratio of input voltage and input impedance. Positive and negative sequence of rotor current can be calculated on the basis of equal voltage E_p: $Z_{rp}I_{rp}=Z_pI_s$, and E_n respectively $Z_{rn}I_{rn}=Z_nI_s$. Then:

$$I_{rp} = \frac{Z_pI_s}{Z_{rp}} \quad (5)$$

$$I_{rn} = \frac{Z_nI_s}{Z_{rn}} \quad (6)$$

Torque is defined as difference between its components for forward and backward rotating fields (Fig. 1)

$$T = \frac{p}{\omega}\left(I_{rp}^2\frac{0{,}5R_r'}{s} - I_{rn}^2\frac{0{,}5R_r'}{2-s}\right) \quad (7)$$

From eq. (1)-(7) can be seen that parameters R'_r, X'_r, X_m, R_s, X_s are needed to be able to simulate torque in steady-state condition as well as in transients (see chap. IV.)

II. Methods for Parameters Determination

There are several methods for SPIM parameters determination that differ in accuracy and procedure. It should be noted that parameters of direct branch of equivalent circuit are measured in the same manner in every presented method by means of locked-rotor test [2]. The most problematic task is determination of magnetizing reactance X_μ and the methods differ from each other in determination of this parameter as it will be discussed below.

A. Classical Method

This method is the most common for measurement of symmetrical three-phase machines. First, resistances of main and auxiliary phase are measured by a DC current test based on the Ohm´s law. Subsequently, a locked rotor test is done. After this measurement all elements of direct branch (R_s, R_r', X_s, X_r') of equivalent circuit (Fig. 4) are detected (see Table II).

It is inevitable to carry out the no-load test for determination of magnetizing reactance X_m, i.e. by no load shaft when motor speed is almost synchronous (a subscript *NL* will be used). Voltage V_s, current I_{NL} and active power P_{NL} are measured again. On these conditions slip is nearly equal to zero. Then Z_p can be viewed as infinite and we can take into consideration only Z_n (Fig. 5).

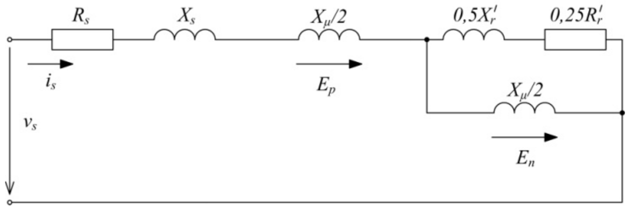

Fig. 5. A single-phase equivalent circuit under no-load condition

Further it is necessary to determine no-load losses and to extract active part of the no-load current. After that the magnetizing current can be determined and magnetizing reactance calculated as follows:

$$X_\mu = \frac{2E_p}{I_\mu} \tag{11}$$

The result is in Table IV.

B. Suhr's Method

This method, described in [3], is based on measurement of induced voltage in the auxiliary phase.

A digital wattmeter is connected in such a way that no load current I_{NL} of the main winding flows through its current coil and voltage of auxiliary phase is applied to its voltage coil. In such case the wattmeter measures reactive power Q. The reactance X_Q can be now calculated as:

$$X_Q = \frac{Q}{I_{NL}^2} \tag{12}$$

When measuring the input current, voltage and active power by the other wattmeter, the X_0 can be determined as input reactance of main winding. Subsequently we can state:

$$X_Q + X_0 = X_s + X_\mu \tag{13}$$

where X_s can be determined on the basis of locked rotor measurement (see Eq. 10b). Then X_μ will be obtained from the Eq. 13 (see Table IV).

C. Two-Phase Method

This method proposed in [4] supposes connecting and feeding the auxiliary phase. The following conditions are to be followed: magneto-motive force (MMF), which means the winding current multiplied by number of effective turns, has to be the same in both phases and the currents are to be shifted by 90°. If the above mentioned conditions are kept the backward field of main winding is entirely eliminated and field produced in air gap is uniform and similar to the field produced in three-phase machines. Thus, the equivalent circuit is simplified as illustrated in the Fig. 6.

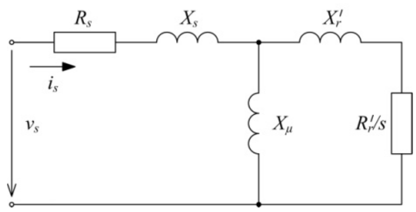

Fig. 6. Equivalent circuit for symmetrical two-phase operation.

The parameters can then be easily measured like in the three-phase machines (see Table IV).

D. Finite Element Method (FEM)

As mentioned above, the most complicated task seems to be a determination of magnetizing reactance. For its determination is possible to apply also the FEM [7] by means of no-load simulation test. The simulation is carried out at zero frequency assuming to work in rotor reference frame. This corresponds to a rotor slip *s* equal to zero (Fig. 7). Stator currents are imposed in the model and the non-linear behavior of magnetizing inductance vs. current is computed.

Total energy stored in the magnetic circuit W_{AJ} is computed as a sum of magnetic energy and coenergy. After FEM analysis the magnetizing inductance can be calculated as follows:

$$L_\mu = \frac{W_{AJ}}{I_{NL}^2} \tag{14}$$

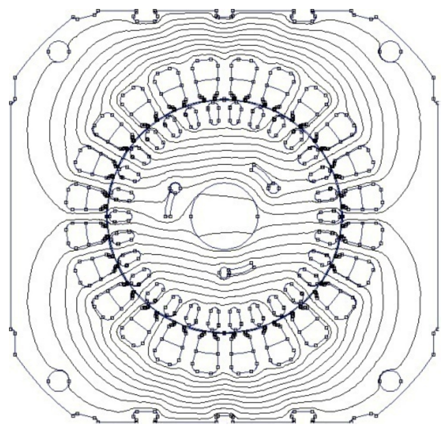

Fig.7. Cross-section of investigated SPIM for FEM analysis.

E. Calculations

If the material constants and geometry dimensions of the machine are known it is possible to calculate all these parameters on the basis of design of electrical machine to confirm previous results. All calculations were done by equations according to [5] and due to lack of space only results are presented here (Table I).

TABLE I
CALCULATED PARAMETERS OF THE MACHINE

X_s (Ω)	L_s [H]	X'_r (Ω)	L'_r [H]	X_μ (Ω)	L_μ [H]
19.82	0.0631	26.95	0.0858	315.6	1.0046

As the investigated machine has the same slots and coils the calculated parameters are valid also for main and auxiliary winding.

III. PARAMETERS MEASUREMENT RESULTS

The application of the above mentioned methods has been carried out at a real symmetrical ($N_m = N_a$) two pole SPIM with the followed ratings:

TABLE II
NAMEPLATE OF INVESTIGATED MACHINE

P_N [W]	V_N [V]	n_N [rpm]	I_N [A]	T_N [Nm]
150	230	2730	1.0	0.55

At first, parameters of direct branch of equivalent circuit have been determined. The parameters are in Table II. Resistances have been measured at laboratory temperature and are referred to 20°C.

TABLE II
PARAMETERS OF DIRECT BRANCH OF EQUIVALENT CIRCUIT OF EACH PHASE

MAIN WINDING	R_s [Ω]	R'_r [Ω]	X_s [Ω]
	19,92	50,1	21,37
	X'_r [Ω]	L_s [H]	L'_r [H]
	21,37	0,0679	0,0679
AUXILIARY WINDING	R_s [Ω]	R'_r [Ω]	X_s [Ω]
	21,32	51,1	22,3
	X'_r [Ω]	L_s [H]	L'_r [H]
	22,3	0,0709	0,0709

Table IV shows comparison of magnetizing inductances gained via all proposed methods.

TABLE IV
MAGNETIZING REACTANCES AT NOMINAL VOLTAGE

MEASUREMENT METHOD	X_μ [Ω]	L_μ [H]
CLASSICAL	374.9	1.1933
SUHR'S	233.5	0.7417
TWO-PHASE	452	1.4388
FEM	395.8	1.2599

Afterwards, parameters of equivalent circuit were used in SPIM simulation model for 5 different measurement methods to verify them in motor operation and to find out the torque vs. speed waveforms.

IV. SIMULATION MODEL

For purposes of analysis, the single-phase induction motor can be considered to be an unsymmetrical two-phase machine. The analysis of such machines can be conveniently handled by the normal *d-q* model approach used for three-phase machines. Details of the derivation of the *d-q* model are described in [6]. If all *q* quantities are referred to the main winding and all *d* quantities are referred to the auxiliary winding and all rotor quantities are referred to stator side the voltage equations can be expressed as:

$$v_{qs} = \frac{d\psi_{qs}}{dt} + R_{qs} i_{qs} \tag{15}$$

$$v_{ds} = \frac{d\psi_{ds}}{dt} + R_{ds} i_{ds} \tag{16}$$

$$v_{qr} = \frac{d\psi_{qr}}{dt} + R_{qr} i_{qr} - \frac{N_m}{N_a}\omega_r \psi_{dr} \tag{17}$$

$$v_{dr} = \frac{d\psi_{dr}}{dt} + R_{dr} i_{dr} + \frac{N_a}{N_m}\omega_r \psi_{qr} \tag{18}$$

Flux linkages can be written as:

$$\psi_{qs} = L_{sm} i_{qs} + L_{\mu m}\left(i_{qs} + i_{qr}\right) \tag{19}$$

$$\psi_{ds} = L_{sa} i_{ds} + L_{\mu a}\left(i_{ds} + i_{dr}\right) \tag{20}$$

$$\psi_{qr} = L_r i_{qr} + L_{\mu m}\left(i_{qs} + i_{qr}\right) \tag{21}$$

$$\psi_{dr} = L_r i_{dr} + L_{\mu a}\left(i_{ds} + i_{dr}\right) \tag{22}$$

where R_{qs}, R_{ds}, R_{qr}, R_{dr} are resistances of main and auxiliary winding of stator and rotor (referred to stator side) respectively. L_{sm}, L_{sa} are stator leakage inductances of main and auxiliary winding and L_r is rotor winding leakage inductance. L_{mm} and L_{ma} are mutual inductances between main and auxiliary windings and the identical rotor windings. N_a and N_m are number of turns for auxiliary and main phase respectively. Naturally, for single-phase machine with symmetrical stator windings it is $N_a = N_m$.

In the case of squirrel-cage rotor the rotor voltages in *d* and *q* axes are equal to zero, thus:

$$v_{qr} = v_{dr} = 0 \tag{23}$$

If $_r$ is angular displacement between stator and rotor axes, then

$$\omega_r = \frac{d\vartheta_r}{dt} \tag{24}$$

is angular speed of the rotor.

An expression for the instantaneous electromagnetic torque can be obtained by applying the principle of virtual displacement. This relation (positive for motor action) is expressed as:

$$T_e = p\left(\frac{N_a}{N_m}\psi_{qr}i_{dr} - \frac{N_m}{N_a}\psi_{dr}i_{qr}\right) \qquad (25)$$

where p is a number of pole-pairs. The simulated results are seen on the Fig. 9, 10, 11, 13, 14.

V. Experimental Results

Measurements have been made by two reasons: as first to verify the parameters (Chapter III) and second to verify the simulated waveforms of torque and current vs. speed. To verify the simulated results the behaviour of the machine under various load conditions was investigated by a mechanical coupling of the investigated machine to permanent magnet DC machine via torque transducer MBM T20WN (Fig. 8).

Consequently, a comparison between simulated and measured torque-speed characteristic was done.

A. SPIM supplied only to main phase

This connection of single-phase machine has only educational importance and it is not used in praxis. Thus, simulations of this kind of SPIM supplying are omitted and our effort was focused on other possible connections.

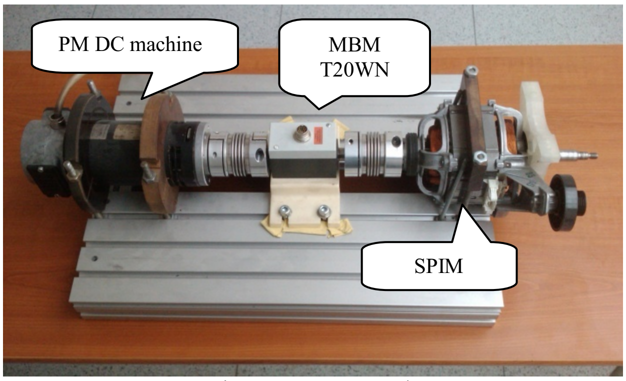

Fig. 8. Motor test stand.

B. SPIM with capacitor

This connection is done by connecting the capacitor to auxiliary phase. Stator voltage in d axis can be now written:

$$v_{ds} = v_s - \frac{1}{C}\int i_{ds}dt \qquad (26)$$

where v_s is the supply voltage and C is the capacity of the capacitor.

SPIM with capacitor (Fig. 2b) is the most common connection. Phase shift between main and auxiliary phase causes unsymmetrical field in machine air gap what results in oscillated torque-speed characteristic from simulation. It can be approximated by single curve (Fig. 9) which will be used in further figures to compare it with measured curve.

Furthermore, simulated torque-speed characteristics can be compared to the torque-speed characteristic measured on real machine to evaluate the most accurate parameters measurement method (Fig. 10). Best agreement was gained between measurement and simulation with parameters from Suhr's method. Naturally, small difference between measured and simulated torque can be caused by idealities in simulation model.

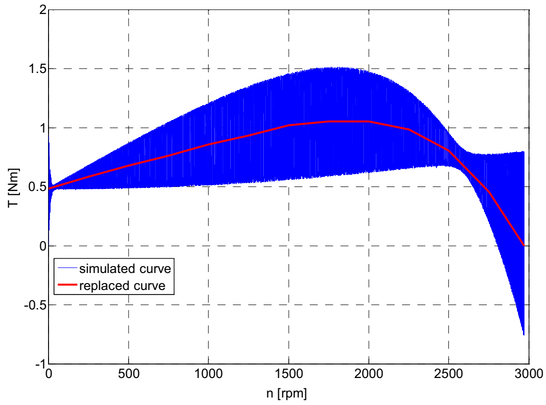

Fig. 9. Simulated torque-speed characteristic and its approximation.

Good agreement between measurement and simulation has been achieved also in main and auxiliary currents as a function of motor speed (Fig. 11). Thus, the simulation approach seems to be correct and appropriate for determination of SPIM parameters.

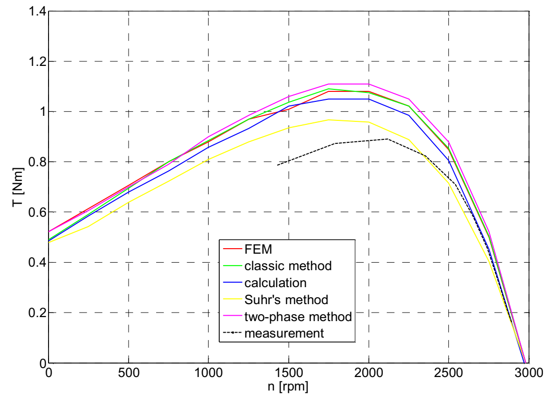

Fig. 10. Comparison between measured and simulated torque-speed characteristics of SPIM with capacitor.

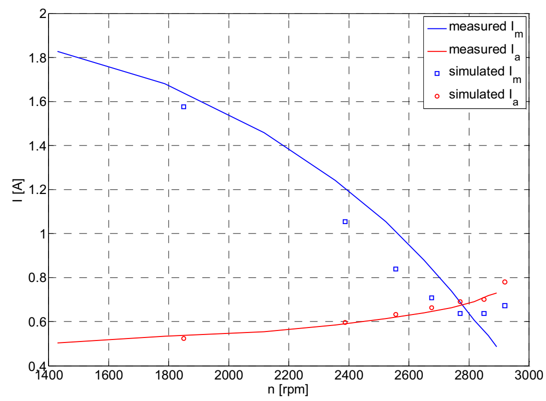

Fig. 11. RMS currents in main and auxiliary phase of SPIM with capacitor.

C. *Two-phase supply of SPIM*

The best performance of SPIM is achieved when it is supplied by two-phase supply [8]. The backward field is fully suppressed and magnetic field in machine air gap is symmetrical.

The same conditions can be achieved also by feeding via two autotransformers with common neutral point and regulated capacitor in series with auxiliary winding (Fig. 12).

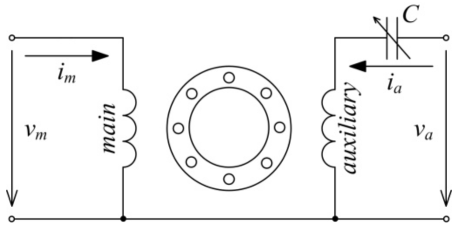

Fig. 12. Two-phase supply for converter compensation.

Keeping magnitudes of main and auxiliary currents equal to each other and phase shift between them equal to 90° the conditions in machine with symmetrical windings are very similar to the conditions when supplied by two-phase supply. This connection is accurate enough for steady-state analysis but not for transients. Thus, it is not practical to use this regulation strategy. However, this method is sufficient for parameters determination and can compensate the two-phase supply.

The torque-speed characteristic is now less oscillated due to the symmetrical magnetic field in machine air gap. This can be seen in Fig. 13.

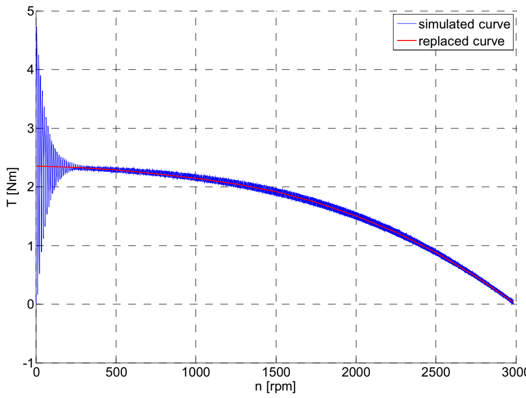

Fig. 13. Simulated torque-speed characteristic for two-phase supply of SPIM and its approximation

Simulated torque-speed characteristics were compared to the torque-speed characteristic measured on real machine supplied by two autotransformers in steady-state conditions (Fig. 14). As can be seen the error is rather small what can be justified by neglected imperfections in simulation model.

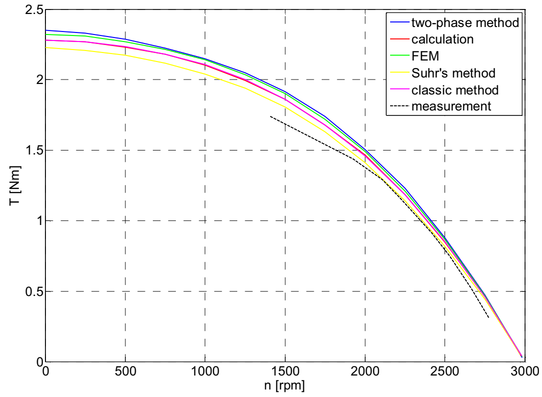

Fig. 14. Comparison between measured and simulated torque-speed characteristics of SPIM with two-phase supply.

VI. Conclusion

In this paper a various methods for SPIM parameters determination have been described. Further, an alternative method for two-phase supply compensation has been proposed. The two-phase supply is replaced by two autotransformers and a variable capacitor to be able to operate and measure the SPIM as a symmetrical three-phase induction machine. This method shows negligible error in steady-states in comparison with two-phase supply and it can be recommended for parameters investigation. The parameters were then used in simulation model of SPIM and simulation results subsequently compared to measurement on SPIM coupled to the PM DC machine via torque transducer. Simulation shows good agreement with measurement and thus the measurement and determination of SPIM parameters can be considered as satisfactory.

VII. References

[1] Hrabovcová, V.; Rafajdus, P.: *Radial Magnetic Forces of Single-Phase Permanent Split-Capacitor Motor,* Journal of Electrical Engineering, vol. 57, July - August 2006, pp. 185-192.

[2] Gross, Ch. A.: *Electric Machines*, CRC Press, 2006, pp. 228 – 229.

[3] Suhr, F.W.: *Towar an Accurate Evaluation of Single-Phase Induction-Motor Constants*, AIEE Power Apparatus and Systems, Vol. 71, 1952, pp. 221 – 227.

[4] Van Der Merve, C.; Van Der Merve, F. S.: *A Study Of Methods to Measure the Parameters of Single-Phase Induction Motors*, IEEE Transactions on Energy Conversion, Vol. 10, Jun 1995, pp. 248 – 253.

[5] Pyrhonen, J.; Jokinen, T.; Hrabovcova, V.: *Design of rotating electrical machines*, John Wiley & Sons, 2008, pp. 221 – 253.

[6] Krause, P. C.: *Simulation of Unsymmetrical 2-Phase Induction Machines*, IEEE Transactions on Power Apparatus and Systems, Vol. 84, Nov. 1965, pp. 1025 – 1037.

[7] Bianchi, N.: *Electrical Machine Analysis Using Finite Elements*, Taylor & Francis, 2007.

[8] Abdel-Rahim, Naser M. B.; Shaltout, A.: *An Unsymmetrical Two-Phase Induction Motor Drive With Slip-Frequency Control*, IEEE Transactions on Energy Conversion, Vol. 24, Sep. 2009, pp. 608 – 616.